Development of a Digital X-Ray Radiography System for BWR Control Blade Inspection

Byungsik Yoon, John Beale, Brenden Mervin, Rob Daum
Electric Power Research Institute (EPRI)
1300 West W.T. Harris Blvd., Charlotte, NC 28262 USA

ABSTRACT

Control blades perform an important safety function in a BWR nuclear plant and must be well maintained to ensure plant safety. Currently, control blades are inspected visually for indications of cracking or other degradation. However, visual inspections are limited in their ability to identify degradation and cannot detect internal defects or neutron absorber washout or depletion. Therefore, volumetric inspection techniques are necessary for it to be possible to assess the integrity of the control blade. Overall, digital X-ray radiography appears to have promise for field application. EPRI developed a digital X-ray radiography inspection system for control blades that can be deployable poolside and has been tested in a simulated poolside environment. This paper describes the development of the X-ray radiography inspection system and presents the results of a poolside demonstration.

1. Introduction

In a nuclear power plant, energy released from the nuclear fission of the fuel generates heat that is used to boil water to produce steam and provide electric power by means of forcing the rotation of a turbine. The nuclear fuel resides inside the reactor pressure vessel (RPV) core. The nuclear reaction that takes place in both boiling water reactors (BWRs) and pressurized water reactors (PWRs) must be carefully maintained during both operation and shutdown to control reactor criticality. This is done by means of control rods in PWRs and control rod blades, also referred to as control blades, in BWRs. Figure 1 shows a small mockup of a BWR control blade.

Control blades contain a neutron absorbing material that is capable of capturing and absorbing thermal neutrons. Control blades are used for shutdown of the reactor, but also control the fission activity and power distribution of the reactor. Typically, the neutron absorbing material is in the form of boron carbide (B_4C) [1]. Control blades must have sufficient absorber materials remaining to be able to safely halt the nuclear fission process as well as maintain subcriticality of the reactor during shutdown by a shutdown margin as defined by the nuclear power plant reactor's technical specification [1]. Therefore, control blades perform an important safety function in a nuclear plant and must be well maintained to ensure plant safety. If damaged or degraded, control blades must be replaced.

Currently, the majority of nuclear power plants are inspecting control blades visually for indications of cracking. Visual testing is performed during an outage by using a remotely controlled radiation resistant underwater camera. However, visual inspection is limited in its ability to identify surface degradation and has no ability to detect internal defects or neutron absorber washout or depletion. Therefore, improved inspection techniques are needed to enable evaluation of the overall health and fitness for service of the control blades.

Recently, several plants have experienced issues related to control blades, primarily in the form of cracking, which causes neutron absorber washout and a reduction in the plant's

margin for maintaining safe shutdown.
For this reason, EPRI has initiated a project to evaluate various inspection technologies and techniques for evaluating the condition of control blades. The ideal inspection technique would have the ability not only to detect structural anomalies related to mechanical end of life (MEOL), but also to detect conditions related to nuclear end of life (NEOL), such as absorber depletion and washout [2]. While x-ray technology cannot detect depletion, it has the potential to determine washout of the absorber material.

2. Mockup Development

Three mockups were utilized in the majority of experiments and technique evaluations performed for this study: one each from two different control blade manufacturers and an x-ray standard with calibrated defects. Both of the control blade mockups were filled with varying amounts and densities of boron carbide, air or water, and hafnium pins. This paper contains experimental results obtained using one specific mockup. Figure 1 shows an image of the control blade mockup referred to in this paper, along with its loading map.

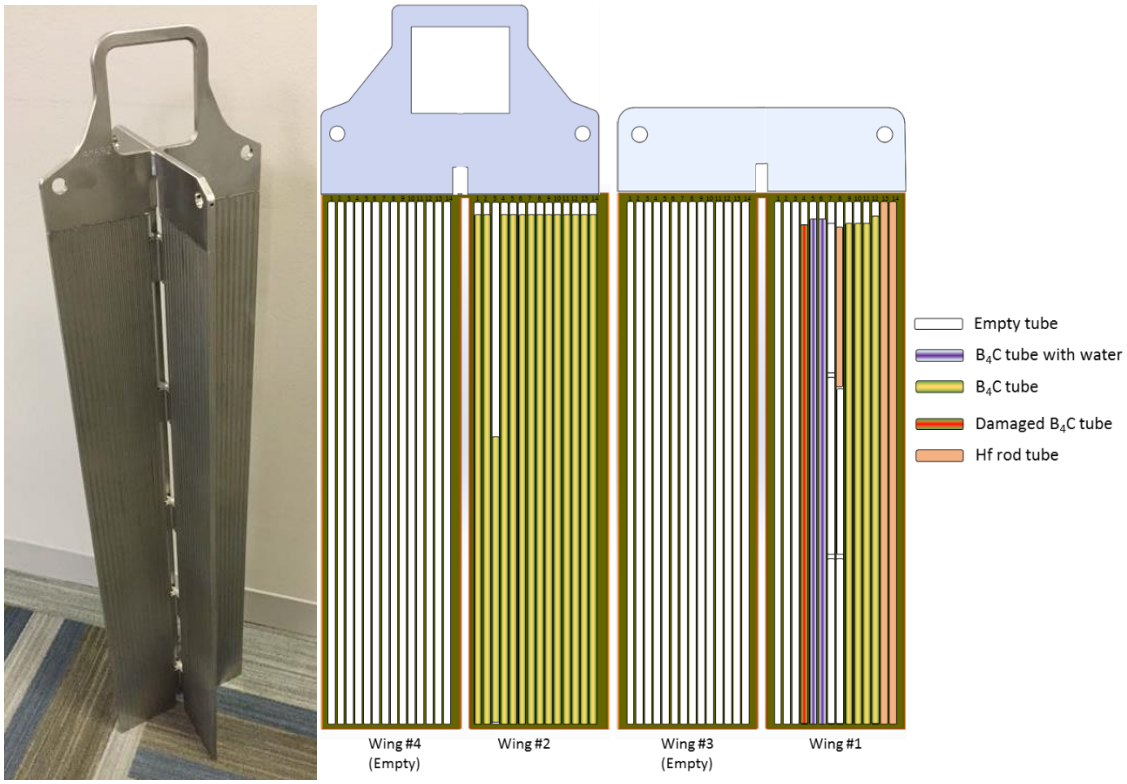

Figure 1. Photo of control blade mockup and loading map

This mockup contained four wings: two filled with various materials and two that were empty. Table 1 presents the materials loaded into the control blade by wing and tube numbers.

Tube No.	Wing 1	Wing 2	Wing 3	Wing 4
1	Empty	Full-length B_4C tube (type C)	Empty	Empty
2	Empty	Full-length B_4C tube (type C)	Empty	Empty
3	Empty	Partial-length B_4C tube (type C)	Empty	Empty
4	Damaged full-length B_4C tube (type A)	Full-length B_4C tube (type C)	Empty	Empty
5	Full-length B_4C tube with water in the tube (type B)	Full-length B_4C tube (type C)	Empty	Empty
6	Full-length B_4C tube with water in the tube (type B)	Full-length B_4C tube (type C)	Empty	Empty
7	3 empty tubes with no B_4C inside (type C)	Full-length B_4C tube (type C)	Empty	Empty
8	2 empty tubes with no B4C inside with one Hf rod at the top end (type C)	Full-length B_4C tube (type C)	Empty	Empty
9	Full-length B_4C tube (type A)	Full-length B_4C tube (type C)	Empty	Empty
10	Full-length B_4C tube (type A)	Full-length B_4C tube (type C)	Empty	Empty
11	Full-length B_4C tube (type B)	Full-length B_4C tube (type C)	Empty	Empty
12	Full-length B_4C tube (type D)	Full-length B_4C tube (type C)	Empty	Empty
13	Full-length Hf rod, smaller diameter	Full-length B_4C tube (type C)	Empty	Empty
14	Full-length Hf rod, larger diameter	Full-length B_4C tube (type C)	Empty	Empty

Table 1. Control blade mockup blade loading table

3. Development of the Digital X-Ray Radiography System

Several techniques were considered for development (e.g. neutron radiography, guided wave) however, digital X-ray radiography was selected as a field-deployable technique due to its cost effectiveness, portability and the reliability of inspection results. Actual inspections will be conducted in an underwater environment, so the digital X-ray system was designed to be waterproof. Figure 2 shows a 3D model of the EPRI-designed underwater digital X-ray radiography system and a photo of the assembled system.

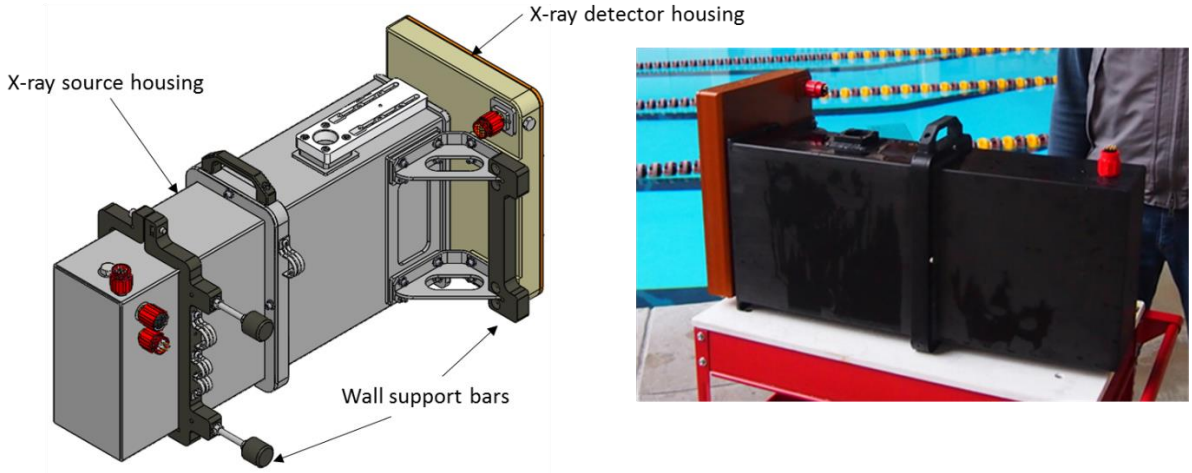

Figure 2. 3D model (left) and assembled (right) digital X-ray radiography system

An X-ray emitter is installed inside the source housing, and an image detector is embedded inside of housing that is separated from the X-ray emitter housing. There is an adjustable

gap between the image detector and the X-ray emitter housing. The control blade is slid through the gap and positioned to be inspected by exposure to X-rays. This inspection system can complete a whole wing by taking several exposures along the vertical length of control blade. A total of 17 exposures is necessary to complete one wing inspection.
A functionality test was conducted in laboratory scale using an image quality check plate and mockup. Figure 3 shows the image quality check result obtained using the check plate. Circular geometries for contrast/gray scale check were investigated from higher thickness to lower thickness to find out the last visible indication. The 11-mm-diameter circles that are arrayed on the upper area of the plate are low-contrast, large-detail check points and can be identified up to 0.5% scale. The 0.5-mm-diameter circles that are arrayed inside of 11-mm circles are high-contrast, small-detail check points and can be observed to 4.5% scale. A gray scale check point located at the lower part of image test object showed maximum gray scale performance. A spatial resolution check area is hard to resolve by the naked eye, so image processing software was involved to measure. The software used for the analysis is ImageJ. A line is drawn to the area that has line pairs and assessed by gray value profile to identify the maximum line pairs per millimeter (LP/mm). All five separated lines are identified at 2.24 LP/mm, but beyond this point the lines were not resolved.

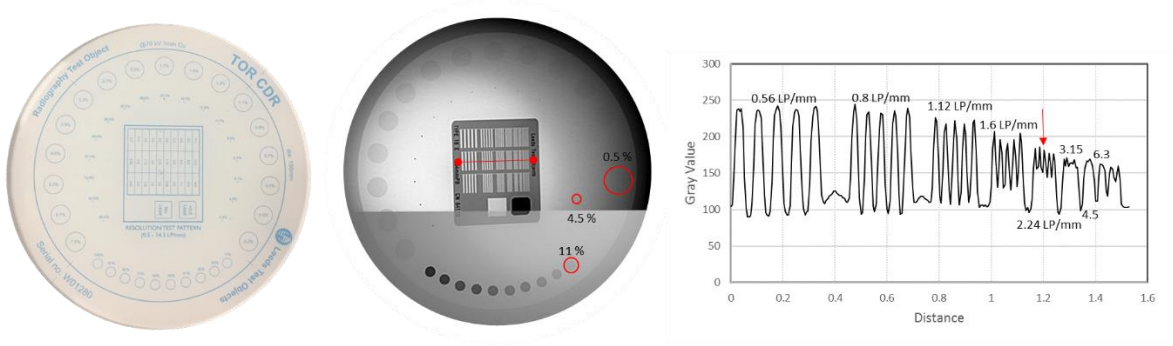

(a) (b) (c)

Figure 3. Image quality and resolution test result using image quality check plate: (a) image quality check plate, (b) radiography image of plate, (c) gray scale profile along with red line in radiography image

4. Poolside Demonstration

The developed X-ray radiography system was tested in a simulated spent fuel pool environment to verify overall performance and check the waterproof function of housing and connectors. The test was conducted underwater at a depth of 6 m using the image quality check plate and EPRI mockup. Figure 4 shows the poolside demonstration performed in the simulated spent fuel pool.

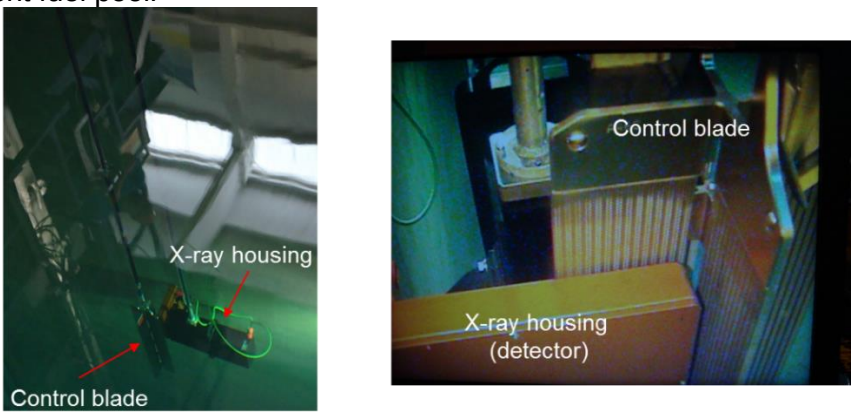

Figure 4. Photos of simulated poolside demonstration

The X-ray system was positioned at a specific location, and then the control blade mockup was moved to the X-ray housing and slid onto the inspection gap. Vertical movement of the control blade mockup was executed by encoded crane. X-ray exposure started with the control blade at a stationary position and moved up the control blade in 200-mm increments for subsequent exposures.

Image averaging was evaluated by setting up three different averaging values. As shown in Figure 5, there is no noticeable difference in radiography images with averaging however averaging may be effective when this system is applied in an actual spent fuel pool inspecting blades with a high background radiation level.

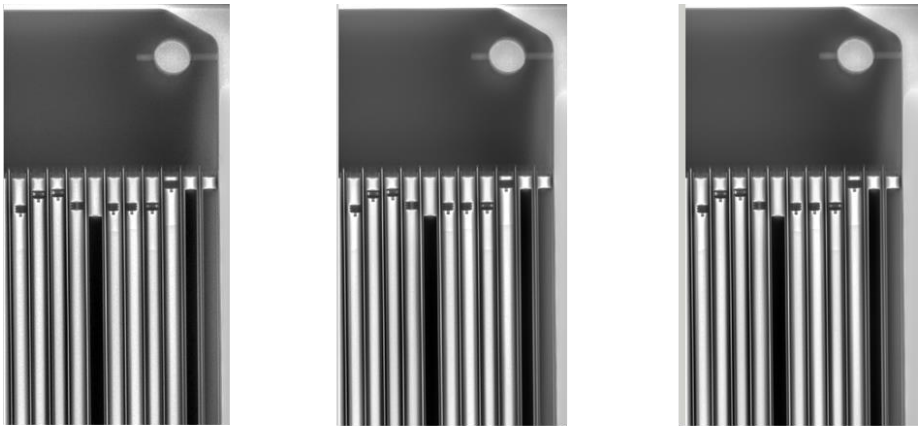

Figure 5. Comparison of radiography images from three different averaging values

To compare the difference of image resolution in laboratory and underwater testing, gray scale values were measured at the same line from the image quality check plate. Figure 6 shows a gray value profile in air and water conditions. As seen on the graph, the same resolution is shown in air and water. However, the contrast ratio measured as peak-valley differences was reduced in water compared with air. This is due to the attenuation of water.

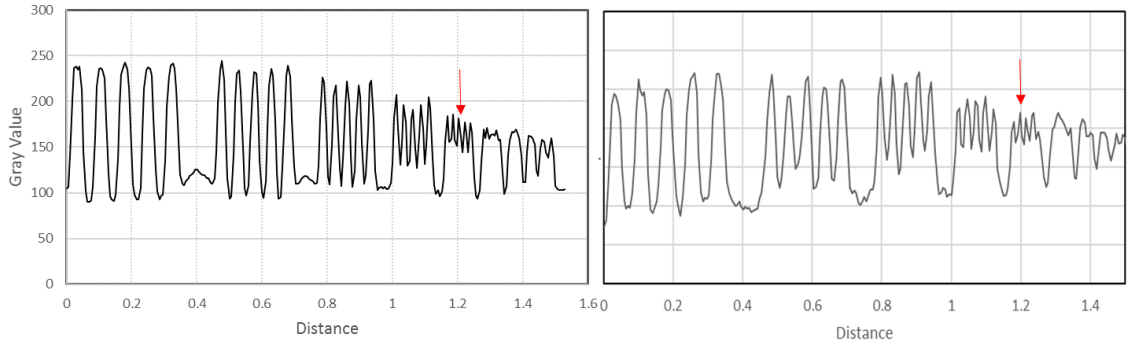

(a) (b)

Figure 6. Comparison of image resolution between air and water: (a) laboratory environment (air), (b) underwater environment (water)

The fabricated underwater X-ray system has 40 cm of separation distance between the X-ray emitter and the detector surface to minimize the overall system size and weight. Due to the proximity of the X-ray emitter and detector, the radiography image shows a cone effect. This close separation distance causes the gradual gray value variance from the center of the image to the edge. The cone effect may reduce the ability to differentiate subtle image changes such as water ingress and air bubbles inside of tubes.

To compensate for the cone effect, a simple image calculation process was adopted, based on a component image divided by a null image taken without any object. Figure 7 shows the gray scale variance across the radiography image and the compensation process. There is about 300% of gray value difference existing between the center and the top of the image. However, the compensated image shows quite uniform gray scale across the image. The compensated radiography image can provide quantitative evaluation regarding boron absorber washout and damaged tubes.

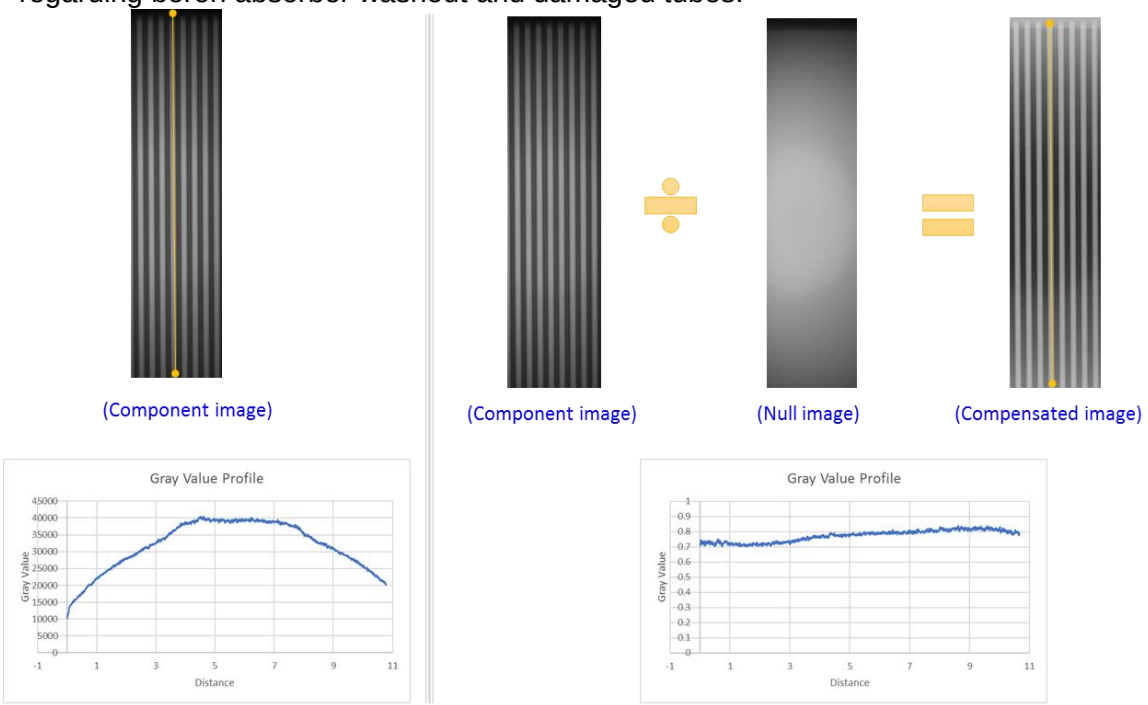

(a) (b)

Figure 7. Gray scale variance compensation process: (a) before compensation (b) after compensation

Figure 8 shows a complete radiography image stitched together with four images taken along with vertical locations of the mockup. As shown in this image, all loading conditions are identified. From this figure, it can generally be seen where B_4C is missing in relation to fill gas, and the B_4C level is easily observable as well. Three air bubbles were identified from the bottom area of the control blade. The gray value was measured along the green line in the zoomed radiography image and plotted. The gray value of air bubbles shows a higher peak compared with B_4C material.

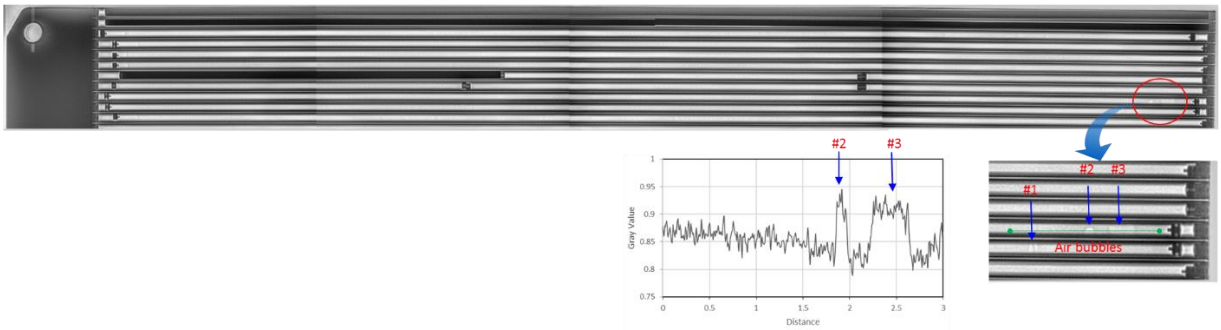

Figure 8. The digitized X-ray image for control blade mockup and zoomed area for the area of observed air bubbles. Gray value plotting for green line across air bubbles.

5. Conclusion

Digital X-ray radiography was chosen as a favorable NDE technique for inspecting control blades in an underwater environment. EPRI developed a digital X-ray camera system for field application and successfully demonstrated it at a simulated spent fuel pool. Performance and operability of the system was verified under water. The system can identify the existence of B_4C from radiography images and identified areas void of B4C in water or air. This means that damaged tubes can be detected and B_4C washout can be identified. However, the effects caused by radiation could not be assessed in this paper. A field demonstration is scheduled in the near future, and the system will be tuned based on field demonstration feedback if available. Additionally, post image processing work may be considered to enhance the quality of radiography images that would be affected by radiation noise.

6. References

1. K.Å. Magnusson and K. Lundgren, “Management of BWR Control Rods,” ANT International, 2011.
2. *Feasibility Study for Control Rod and Control Blade Inspection Techniques.* EPRI, Palo Alto, CA: 2016. 3002007804.